DOI: 10.24850/j-tyca-2021-02-03

Articles

Physical and numerical modeling of focused wave interactions with a low mound breakwater

Modelado físico y numérico de la interacción de ondas enfocadas con un dique vertical con banqueta baja

B. Rodrigo Covarrubias-Contreras[1], ORCID: https://orcid.org/0000-0003-0297-176X

Alec Torres-Freyermuth[2], ORCID: https://orcid.org/0000-0003-0203-8734

José López-González[3], ORCID: https://orcid.org/0000-0002-9977-3104

[1]Laboratorio de Ingeniería y Procesos Costeros, Instituto de Ingeniería, Universidad Nacional Autónoma de México, Sisal, Yucatán, Mexico, BCovarrubiasC@iingen.unam.mx

[2]Laboratorio de Ingeniería y Procesos Costeros, Instituto de Ingeniería, Universidad Nacional Autónoma de México, Sisal, Yucatán, Mexico, ATorresF@iingen.unam.mx

[3]Laboratorio de Ingeniería y Procesos Costeros, Instituto de Ingeniería, Universidad Nacional Autónoma de México, Sisal, Yucatán, Mexico, JLopezGo@ii.unam.mx

Corresponding author: Alec Torres-Freyermuth, ATorresF@iingen.unam.mx

Abstract

Focused waves are a well-known phenomenon that occur in the ocean and can be responsible of offshore structure failure. However, less efforts have been devoted to improve its understanding in the nearshore. This work aims to investigate low-mound breakwater structure stability and functionality associated to transient wave groups. Laboratory experiments were conducted in a wave flume. Free-surface elevation, pressures, and overtopping measurements were employed to validate a numerical model based on the RANS equations. The numerical model predicts the pressures and overtopping with an average relative error of 10% and 8%, respectively. Subsequently, the numerical model was employed to evaluate the role of the relative structure position with respect to the theoretical focused point. Finally, the physical model results are compared with semi-empirical formulations, finding significant differences for both wave overtopping (≈100 %) and pressure/sub-pressure (88 %) estimates. This work demonstrates that RANS models are an alternative to the classic formulations that failed to predict stability and functionality during these phenomena.

Keywords: focused waves, rouge waves, vertical breakwater, structure functionality, structural stability, RANS equations, overtopping.

Resumen

Las ondas enfocadas, fenómeno que ocurre en el océano, son responsables del fallo de estructuras localizadas costa afuera. Existen pocos trabajos enfocados en su estudio en zonas cercanas a la costa. En el presente trabajo se analizó la estabilidad y funcionalidad de un dique vertical con banqueta baja en presencia de ondas enfocadas. Para ello, se realizaron ensayos en un canal de oleaje. Mediciones de superficie libre, presiones, subpresiones y rebase fueron utilizadas para validar un modelo numérico que resuelve las ecuaciones RANS. Las predicciones de rebase y presiones/subpresiones máximas del modelo numérico presentaron diferencias promedio con respecto a las mediciones de 10 y 8 %, respectivamente. De manera posterior, el modelo numérico se utilizó para evaluar el papel de la posición relativa de la estructura. Por último, se compararon los resultados del modelo físico con formulaciones semiempíricas, y se encontraron diferencias significativas en rebase (≈100 %), y en presiones y subpresiones (88 %). Este estudio demuestra que el uso de modelos tipo RANS es una alternativa a las clásicas formulaciones semiempíricas, pues se comparan mejor con las mediciones durante este tipo de fenómenos.

Palabras clave: ondas enfocadas, dique vertical con banqueta baja, funcionalidad, estabilidad estructural, ecuaciones RANS, rebase.

Received: 11/03/2020

Accepted: 29/06/2020

Introduction

The coastal zone is highly vulnerable to both extreme wave events and sea level rise associated to climate change (Gornitz, 1991). Coastal structures are aimed to reduce coastal hazards and allow economical activities in the coastal areas (e.g., tourism, transportation, fisheries, etc.). Thus, knowledge of the mean and extreme wave climate is important in the design of coastal structures (ROM 0.0). The structure design must fulfill the functionality and stability requirements according to the return period (Goda, 2004).

Sea waves are a stochastic phenomenon that can be characterized in both the frequency and time domain. Using spectral wave parameters, we are able to generate an infinite number of time series since phase information is lost from the original time series (Palemón-Arcos, Torres-Freyermuth, Pedrozo-Acuña, & Salles, 2015). However, phase information can be relevant to determine the occurrence of extreme wave events. An example of such interaction are the so-called focused waves which occurs due to constructive interference between individual waves.

These waves are very unpredictable and known as "rogue waves" (Stagonas, Buldakov, & Simons, 2018). Rogue waves in the records show a solitary-like shape with significant wave assymetry (Van-den-Boomgaard, 2003). The rogue wave events can be identified when the wave height exceeds 1.8 times the significant wave heights (Nikolkina & Didenkulova, 2011).

Previous work on focused waves interaction with structures have been mainly focus in deep to intermediate water depth using physical (Ryu & Chang, 2008) or numerical (Amarachaharam, 2016; Palemón-Arcos, Torres-Freyermuth, Chang, Pastrana-Maldonado, & Salles, 2014; Li, Zhao, Ye, Lin, & Chen, 2018) models. The latter can be ascribed to structural damage reported in deep water infrastructure related with petroleum industry. However, few efforts have been devoted to investigate focused waves interaction with coastal structures until more recently (Whittaker *et al*., 2017; Whittaker, Fitzgerald, Raby, Taylor, & Borthwick, 2018). Whittaker *et al*. (2017) and Whittaker *et al*. (2018) demonstrated the important role of focused waves on wave overtopping and forces over coastal structures. These studies were focused on beaches and sloping structures using a Boussinesq model. Thus, the capabilities and limitations of either more advance numerical (e.g., RANS) and simplified (e.g., semi- analytical/empirical) models to quantify the functionality and stability of different typologies require further investigation.

Physical models (Jiménez, 2010; Guanche, 2007) and semi-empirical/ parametric models (Goda, 1974; Franco & Franco, 1999) are often employed for the design of coastal structures. More recently,

numerical models based on the Reynolds-Averaged Navier-Stokes (RANS) equations (Lara, García, & Losada, 2006; Losada, Lara, Guanche, & González-Ondina, 2008; Guanche, Losada, & Lara, 2009; Higuera, Lara, & Losada, 2014; Palemón-Arcos *et al*., 2015), able to resolve non-linear wave transformation including wave breaking, have been employed for the design. The current work is aimed to analyzed the stability and functionality of a focused wave interaction with a low-mound breakwater by means of both physical and numerical models. The results are employed to assess the use of semi-empirical and parametric models traditionally employed for the prediction of stability and wave overtopping.

Methods

We adopt an integrated approach consisting on laboratory experiments, numerical modelling, and the use of semi-analytical models to investigate pressure field and overtopping associated to focused waves. A detailed description of each component is given below based on the framework shown in Figure 1.

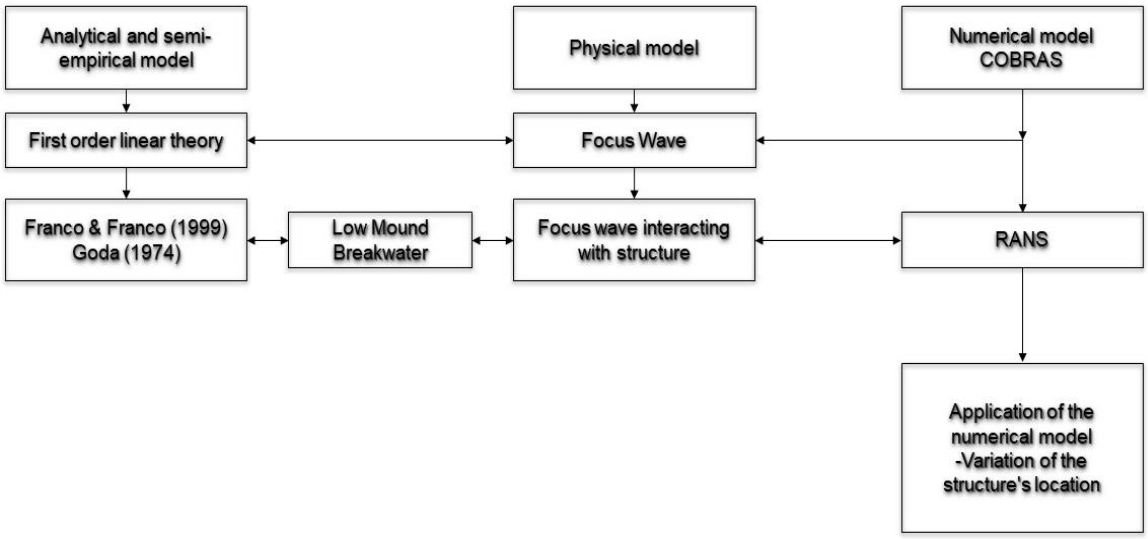

Figure 1. Schematic of the framework for the study of focused wave interaction with a low mound breakwater using physical and numerical and simplified models.

Focused wave generation

Linear wave theory is employed to generate focused waves following prior studies (Longuet-Higgins, 1974; Rapp & Melville, 1990; Baldock, Swan, & Taylor, 1996; Baldock, 2006, among many others). The wave spectrum considers N frequency components containing the same energy to allow constructive interaction (i.e., wave focusing), and hence generating a large wave. The free-surface elevation time series is given by:

$$\eta(x,t) = \sum_{i=1}^{N} a_i \cos(k_i x - \omega_i t - \phi_i) \quad (1)$$

where a_i is the wave amplitude, k_i is the wave number, $\omega_i = 2\pi f_i$ is the angular frequency, ϕ_i is the phase, N is the total number of frequency components and t is the time. The k_i and ω_i are related by the linear dispersion equation ${\omega_i}^2 = g k_i \tanh(k_i h)$, where g and h are the gravity and water depth, respectively. The phase for each component fulfill the following constraint:

$$\cos(k_i x - \omega_i t - \phi_i) = 1 \quad (2)$$

where $x = x_f$ is the wave focusing location and $t = t_f$ is the wave focusing time, re-writing equation (2) as:

$$\phi_i = k_i x_f - \omega_i t_f \quad (3)$$

We obtain that the free-surface elevation time series, by substituting (3) in (1), which is given by:

$$\eta(x,t) = \sum_{i=1}^{N} a_i \cos(k_i(x - x_f) - \omega_i(t - t_f)) \quad (4)$$

where the mean wave paddle position is located at $x = 0$ (Figure 2c) and the water wave displacement at this location is given by:

$$\eta(0,t') = \sum_{i=1}^{N} a_i \cos(-k_i x_f - \omega_i t') \quad (5)$$

where $t' = t - t_f$, and the variations of t_f results in the delay or advance of the focusing time without changing the focusing location x_f.

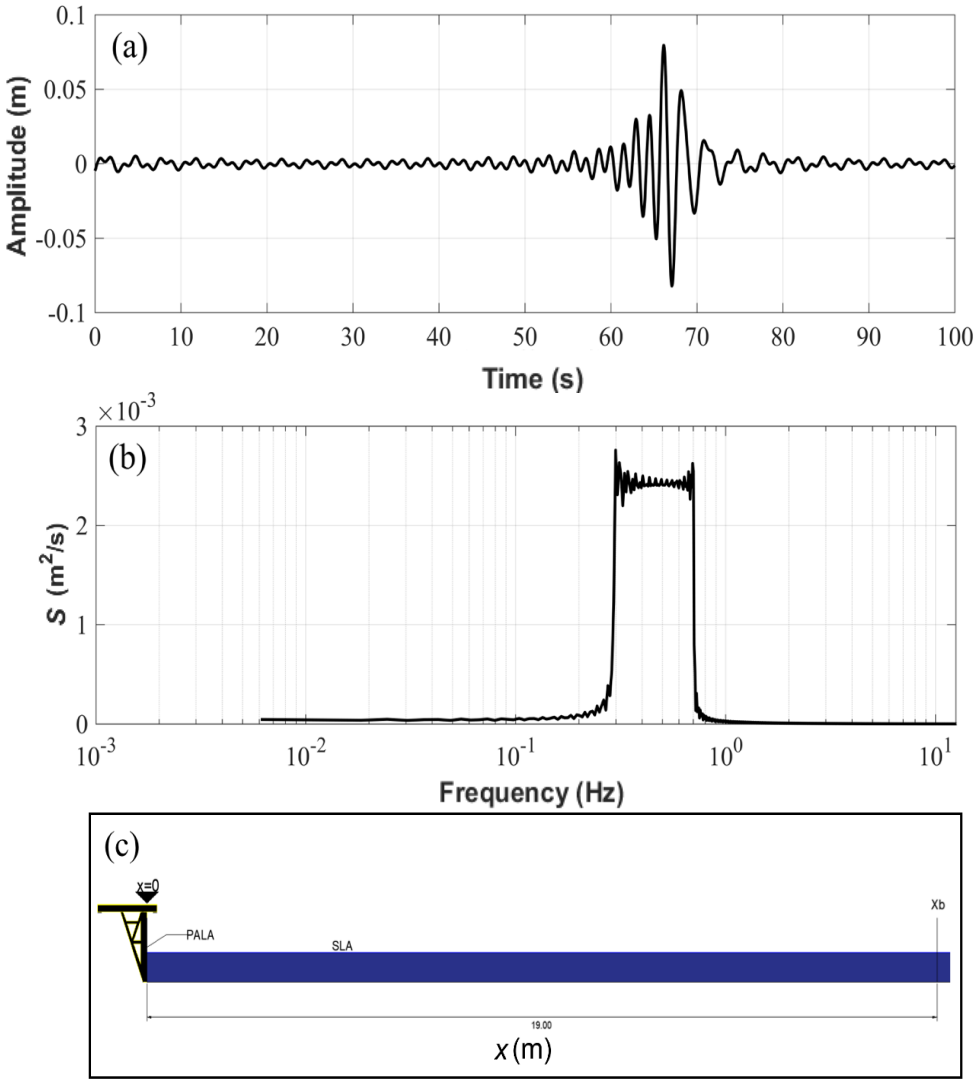

Figure 2. (a) Transient wave group based on 32 primary wave components and specified by $f_c = 1$ Hz, $f_1 = 0.3$ Hz, $f_2 = 0.7$ Hz and $A =$

0.06 m with x_f =19 m; (b) Surface elevation energy spectra; (c) Wave flume and reference system employed during the experiments with origin ($x = 0$ m) at the paddle position.

A transient-focused wave group was generated employing 32 primary wave components (Figure 2a). Prior studies (Rapp & Melville, 1990; Baldock *et al*., 1996; Baldock, 2006) suggest a good representation when using approximately 30 components. The central $f_c = 0.5\,Hz$, lower $f_1 = 0.3\,Hz$, and upper $f_2 = 0.7\,Hz$ frequency limits were used to generate a "top hat" frequency spectra (see Figure 2b). The theoretical wave focusing location was set at $x = 19$ m (Figure 2c) for t_f =100 s.

Physical model

The laboratory experiments were carried out in the wave flume belonging to the Coastal Processes and Engineering Laboratory (LIPC) at the Institute of Engineering (II) of the National Autonomous University of Mexico (UNAM) Sisal Campus. The wave flume is 40 m long, 0.8 m wide, and 1.27 m high (Figure 3). The wave flume is equipped with a 7.5 KW piston-type wave maker from VTI with a paddle stroke of 1.2 m. The waves were generated using simultaneous second-order wave generation

and active wave absorption from a target free-surface elevation time-series derived from (5) and shown in Figure 2a.

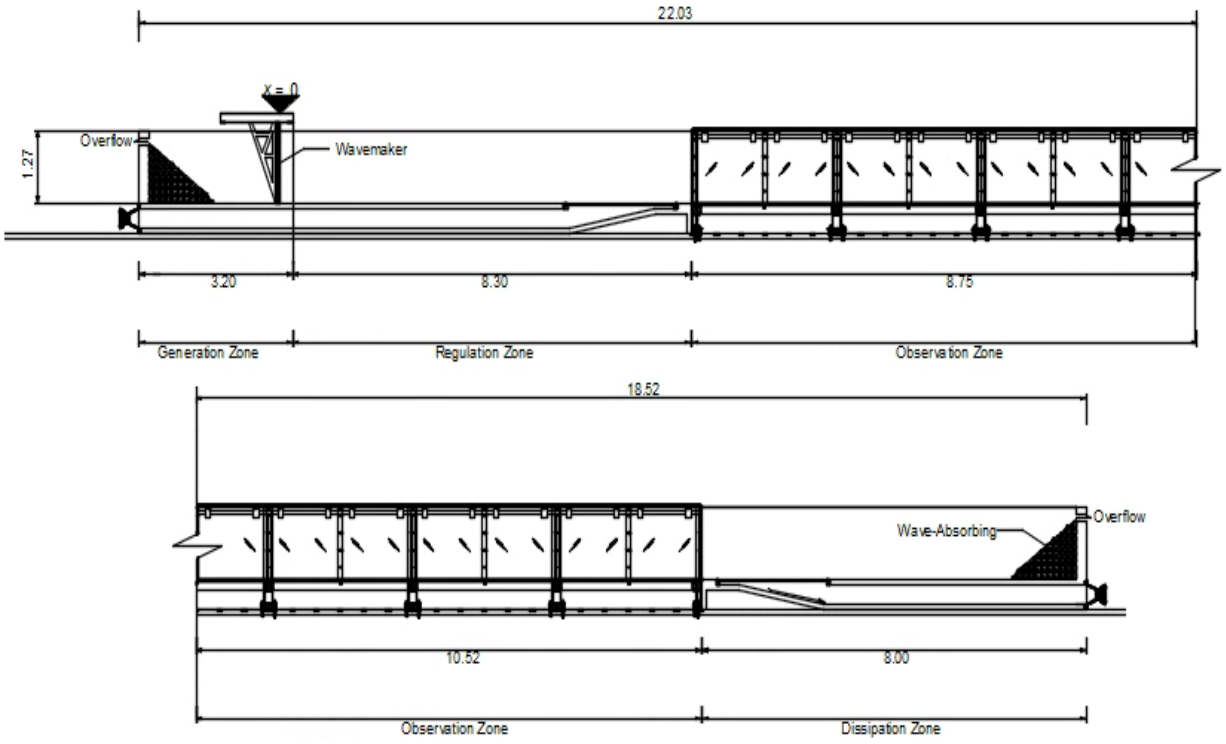

Figure 3. Wave flume cross-section.

Structure layout and laboratory experiments

The experiments consist of transient wave group interaction with a low mound breakwater on a 1:20 physical model. The structure consists of an impermeable caisson made of 3/8¨plywood sheets on a rubble mound foundation with a slope of 1:2 (Figure 4). An overtopping reservoir, made of plywood and acrylic sheets, was installed at the leeside of the structure to measure overtopping volume (see Figure 4).

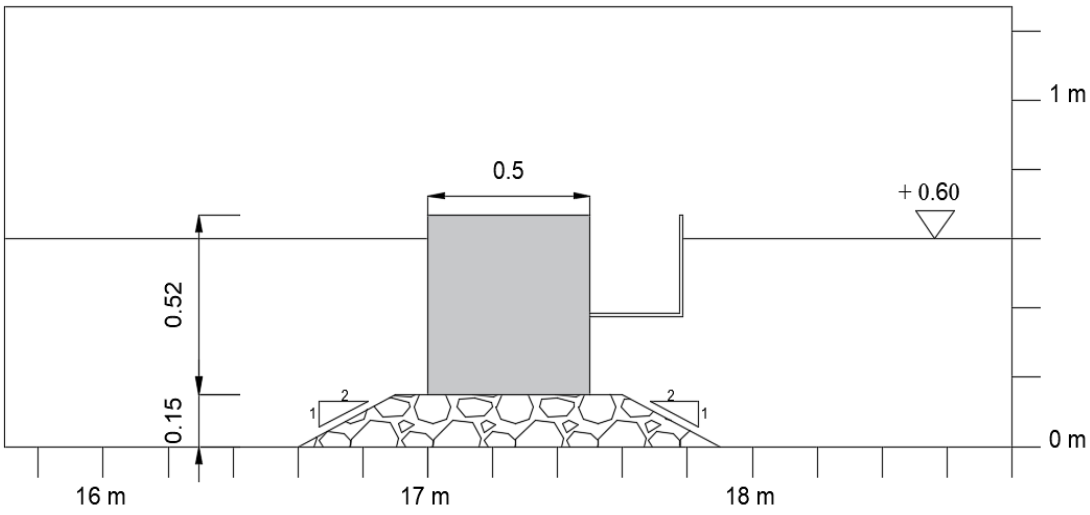

Figure 4. Low mound breakwater and overtopping reservoir cross section.

Physical model tests consist of the following three experiments: (a) transient wave group generation and propagation over uniform water depth (0.60 m) without structure; (b) same water depth and forcing than (a) but with a low mound breakwater at $x = 17$ m; and (c) same wave conditions and structure than (b) but with water depth of 0.50 m. For the

experiments (b) and (c), 15 realizations were carried out to identify to compute ensemble estimates associated to the wave breaking process. The significant wave height (H_s), peak wave period (T_p), and water depth (h) for the simulated cases are specified in Table 1.

Table 1. Experimental tests conducted at the LIPC UNAM wave flume.

Test	h (m)	Wave type	H_s (m)	T_p (s)	Structure location (m)	Realizations
1	0.60	Transient wave group	0.04	2.00	N/A	4
2	0.60	Transient wave group	0.04	2.00	17.00	15
3	0.50	Transient wave group	0.04	2-00	17.00	15

*Where h = water depth; H_s = significant wave height, and T_p = peak wave period.

Data acquisition and analysis

Free-surface elevation time series were collected at 21 cross-shore locations using VTI resistive type wave gauges sampling at 100 Hz (Figure 5). Furthermore, 10 pressure gauges were deployed around the structure to measure pressures along the vertical face and underneath the caisson

(Figure 6). The pressure sensors employed (Keller America) have a precision of ± 0.25 % or ± 0.1 % TEB, pressure range from 0 to 39225.53 Pascals, and temperature range of -10 to 80 °C. The sampling frequency was set equal to 19 Hz for the Tests 2 and 3. On the other hand, wave overtopping was calculated by measuring the water level in the reservoir.

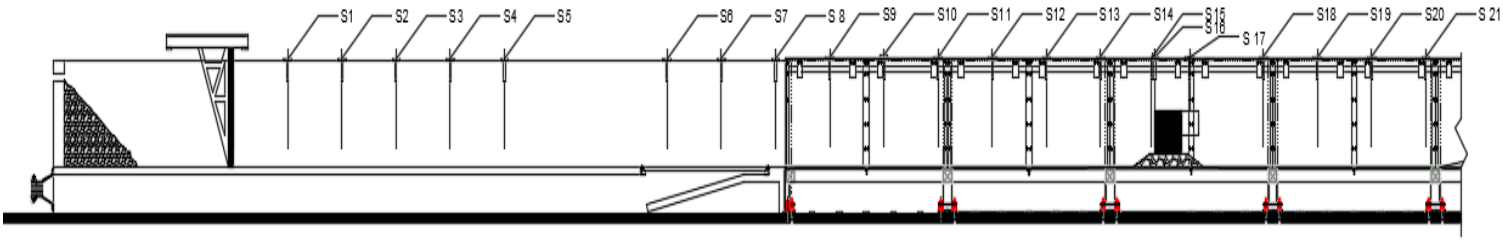

Figure 5. Wave gauges location along the flume for Tests 2 and 3. Test 1 presents the same experimental setup but without the structure.

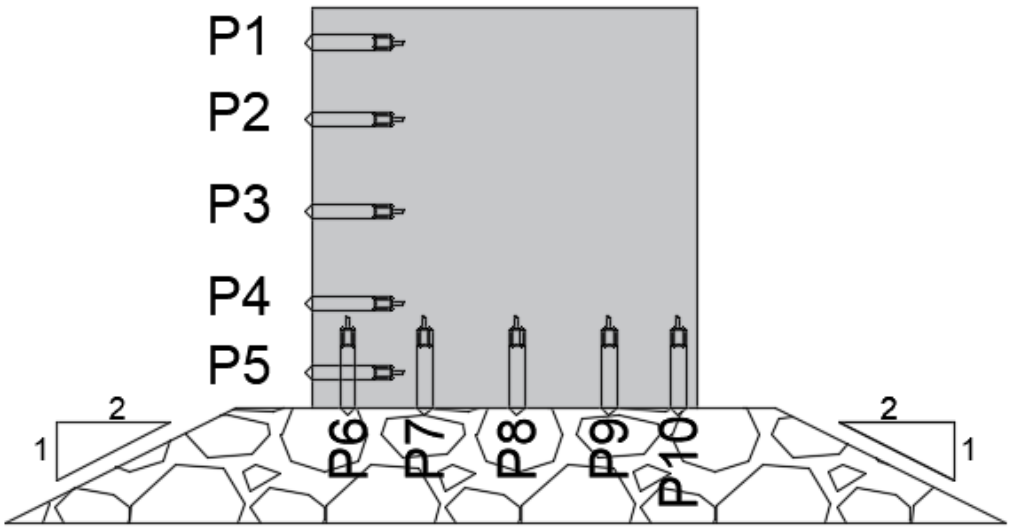

Figure 6. Pressure gauges location along the vertical face and underneath the caisson.

Calibration curves were performed to obtain the calibration coefficients of each sensor to convert from conductance to water surface elevation. Three different still water levels were employed to obtain a linear correlation between voltage and water depth. Mean correlation coefficients were 0.99. Subsequently, a time-domain analysis of waves was conducted using the zero-up crossing method. This allow the identification of individual waves and hence allow us to determine the significant wave height and the maximum wave height at each location. On the other hand, the pressure gauges do not require a calibration and mean and maximum values were calculated from each record. Finally, overtopping was estimated from the recorded water level inside the water reservoir.

Numerical model

The numerical model Cornell Breaking Wave and Structures (COBRAS) (Lin & Liu, 1998) was employed in this work. This model was developed

by Cornell University from the NASA code called RIPPLE. Subsequently, the COBRAS model was adapted for the study of wave-structure interaction for any type of permeable or impermeable structure (Hsu, Sakakiyama, & Liu, 2002; Lara *et al*., 2006; Losada *et al*., 2008).

COBRAS model solves the two-dimensional vertical (2DV) Volume Averaged Reynolds Navier-Stokes (VARANS) equations using a k-ε model. The free-surface is resolve without restrictions by adopting the volume of fluid technique. Therefore, the numerical model is able to simulate complex wave transformation processes during flow-structure interaction including wave reflection, wave breaking, wave transmission, and wave overtopping. The numerical model does not assume any wave theory, reducing the limitations with respect to both non-linear shallow equation (Kobayashi & Wurjanto, 1992) or Boussinesq-type (Chen, Kirby, Dalrymple, Shi, & Thornton, 2003) numerical models.

In the present work, the numerical model is validated with free-surface elevation and pressure time series obtained on a physical model. Moreover, the numerical model is further employed to investigate the role of the relative focusing point location on wave structure functionality and stability. The boundary conditions and computational domain implemented in the numerical model are aimed to reproduce the wave flume experimental facility.

Free-surface elevation time series measured at the offshore sensor (S1 in Figure 5) were employed to force the numerical model. More specifically, the free-surface elevation time series are decomposed into its Fourier components to derive time series of the velocity components employing linear wave theory (Torres-Freyermuth, Losada, & Lara, 2007).

Finally, the horizontal and vertical velocities at the boundary are reconstructed using linear superposition. Active wave absorption is employed in the numerical model to avoid re-reflection at the boundary.

Six simulation were conducted using the RANS numerical model (Table 2). The first case (Case 1) compares the measured and simulated wave focusing location associated with transient wave group propagation over uniform water depth without structure. Case 2 aims to validate the model to investigate wave-structure interaction of the transient wave group with a low mound breakwater. Thus, this case is employed to investigate the model capability to predict complex wave transformation of focused wave interaction, including wave overtopping and pressures, with a structure. Cases 3 to 6 employed the same forcing condition than Case 2 but varied the cross-shore position of the breakwater. These cases allow us to assess the coastal structure stability and functionality sensibility to transient wave groups (see Table 2). For the simulated cases, the model domain was 30 m long and 1.3 high. A uniform mesh with grid resolution of $\Delta x = 0.02$ m and $\Delta y = 0.01$ m and 1500 cells and 130 in x and y directions, respectively. The mesh size was determined from a sensitivity analysis and considering the computational time required.

Table 2. Simulated cases in COBRAS.

Case	h (m)	Wave type	H_s (m)	T_p (s)	Structure location (m)
1	0.60	Transient wave group	0.04	2.00	No structure

2	0.60	Transient wave group	0.04	2.00	17.00
3	0.60	Transient wave group	0.04	2.00	7.00
4	0.60	Transient wave group	0.04	2.00	14.00
5	0.60	Transient wave group	0.04	2.00	20.00
6	0.60	Transient wave group	0.04	2.00	27.00

Semi-analytical and parametric models

We employed existing semi-empirical formulations found in the literature to assess structure stability and functionality of a low-mound breakwater. These formulations were employed to assess the performance of such formulation with respect to physical model measurements

A wave pressure formulae, proposed by Goda (1974), is here employed to evaluate wave pressures along and underneath the structure. The formulation. The model employed the following formulations to estimate the pressures:

$$H = 1.8 * H_{1/3} \quad (6)$$

$$\eta^* = 0.75(1 + cos\beta)H \quad (7)$$

$$p_1 = 0.5(1 + cos\beta)(\alpha_1 + \alpha_2 cos^2\beta)\rho_w g H \quad (8)$$

$$p_2 = \frac{p_1}{\cosh(\frac{2\pi h}{L})} \quad (9)$$

$$p_3 = \alpha_3 p_1 \quad (10)$$

$$p_u = 0.5(1 + cos\beta)\alpha_1\alpha_3\gamma_w H \quad (11)$$

The pressure factors α_i are given by:

$$\alpha_1 = 0.6 + 0.5\left[\frac{4\pi\frac{h}{L}}{senh(4\pi\frac{h}{L})}\right]^2 \quad (12)$$

$$\alpha_2 = min\left\{\left[\frac{h_b - d}{3h_b}\left(\frac{H}{d}\right)^2, \frac{2d}{H}\right]\right\} \quad (13)$$

Where:

$$h_b = h + 5H_{1/3}tan\theta \quad (14)$$

$$\alpha_3 = 1 - \frac{h\prime}{h}\left[1 - \frac{1}{cos(2\pi\frac{h}{L})}\right]^2 \qquad (15)$$

The relevant variables and parameters considered in this model are shown in Figure 7. Table 3 presents the parameters employed for the physical model experiment conducted in this work.

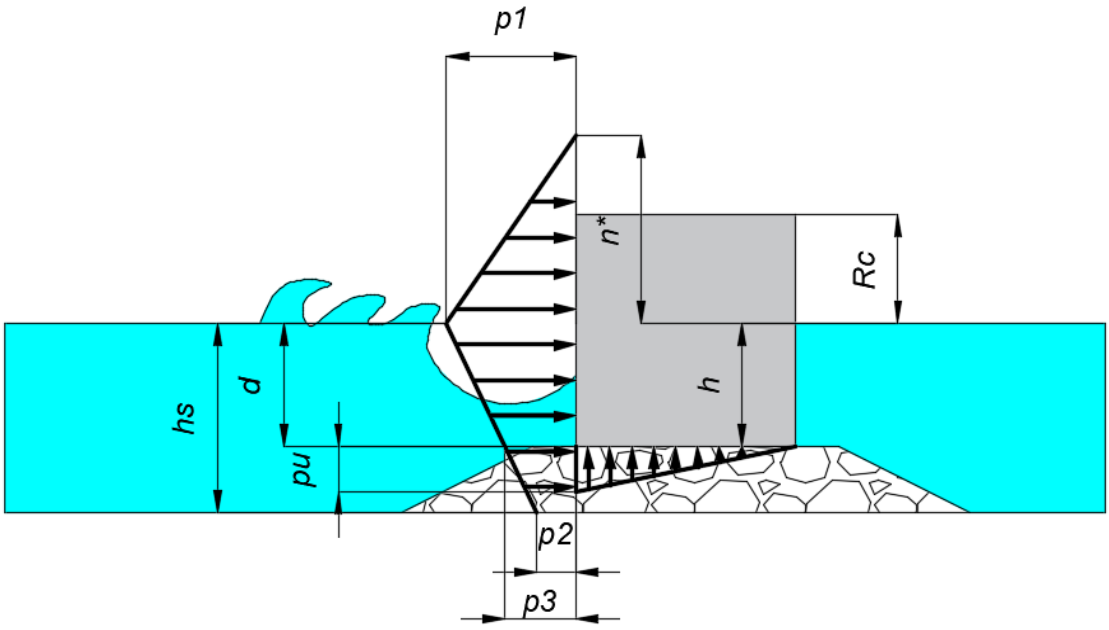

Figure 7. Distribution of design wave pressure proposed by Goda (1974).

Table 3. Parameter values used by the model proposed by Goda (1974).

Test	*hs*	Wave type	H_s	*H*	T_p	*hc*	*h*	*β*

	(m)		(m)	(m)	(s)	(m)	(m)	
2	0.60	Transient wave group	0.04	0.80	2.00	0.07	0.45	0
3	0.50	Transient wave group	0.04	0.80	2.00	0.17	0.45	0

*Where *SW* = water free surface; H_s = significant wave height; T_p = peak wave period; *hs* = water; depth; *h* = draft and β = wave incidence angle (º).

We employed the design formula for wave overtopping on vertical breakwaters proposed by Franco and Franco (1999), which is given by:

$$Q = \frac{q}{\sqrt{gH_s{}^3}} = 0.082\exp(-3.0\frac{Rc}{H_s}\frac{1}{\gamma_\beta\gamma_s}) \quad (16)$$

Where:

Q = dimensionless mean wave overtopping discharge.

q = Caudal medio de rebase ($m^3/s/m$).

g = gravity acceleration (m^2/s).

Rc = freeboard (m).

Hs = significant wave height (m).

γ_β =reduction factor due to wave incidence angle.

γ_s =reduction factor due to structure geometry.

We employed the design formulation proposed by Franco and Franco (1999) with the parameters shown in Table 4.

Table 4. Parameters employed in the formulation by Franco and Franco (1999).

Test	hs (m)	Wave type	Hs (m)	Tp (s)	Rc (m)	γ_β	γ_s
2	0.60	Transient wave group	0.04	2.00	0.07	0.83	1
3	0.60	Transient wave group	0.04	2.00	0.17	0.83	1

Results

Here, the physical model experiments are employed to validate the numerical model to further investigate stability and functionality due to the interaction of a transient wave group with a low mound breakwater.

Subsequently, the numerical model is further employed to investigate stability and overtopping sensibility to the cross-shore location.

Numerical model validation

The numerical model was compared against free surface elevation time series measured across the wave flume, wave pressure around the structure, and wave overtopping.

Wave transformation

Wave focusing for the transient wave group is predicted at $x = 19$ m by linear wave theory (Eq. (5)). However, laboratory observations show that wave focusing occurred at $x = 17$ m for this condition. Figure 8 shows the measured and model predicted free-surface elevation time series at

different cross-flume locations corresponding to Test 1 (without structure) and Test 2 (with structure). The transient wave group transformation is well reproduced by the numerical model in the absence of the structure (Figures 8a-1 and 8b-1), including the wave focusing location (Figure 8c-1). Differences in the wave focusing location found in both the laboratory data and the numerical model with respect to theory suggest that can be ascribed non-linear wave transformation processes. Baldock *et al*. (1996) reported such differences that increase with wave group non-linearity.

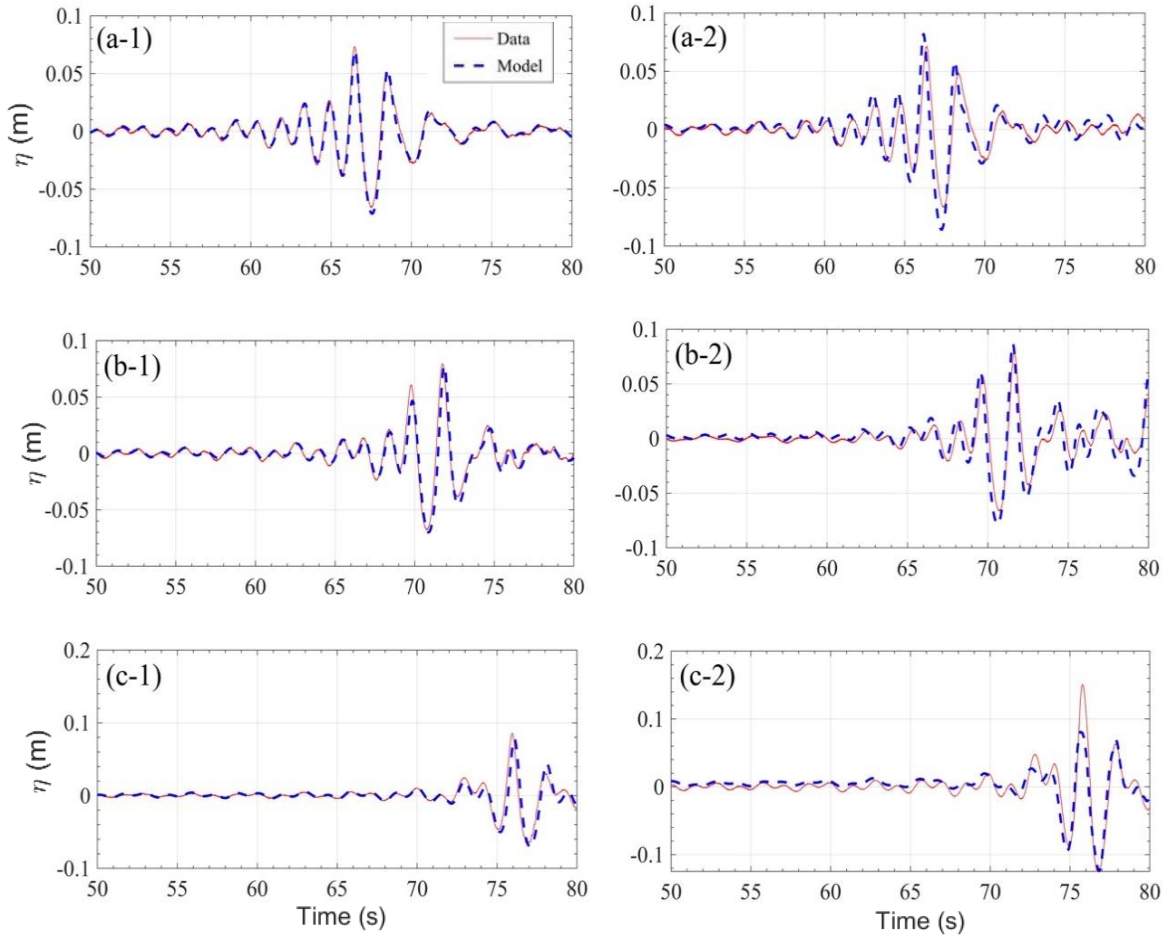

Figure 8. Model-data comparison of free-surface elevation time series at (a) $x = 1$ m; (b) 8 m, and (c) 17 m corresponding to transient wave group transformation (1) without and (2) with the presence of a low mound breakwater at $x = 17$ m.

Figure 8-2 shows the wave transformation in the presence of a low mound breakwater (i.e., Test 2). The numerical model satisfactorily simulates the wave group propagation (Figures 8a-2 and 8b-2). Wave-structure interaction induced wave reflection, breaking, and overttoping. It is worth to notice the increase in the free-surface elevation in front of the structure (Test 2) owing to wave reflection (Figure 8c-2). Moreover, the numerical model predicts the wave asymmetry, whereas the maximum free-surface elevation in front of the structure is under predicted (see Figure 8c-2).

Wave-induced pressures

Wave-induced pressures times series were measured at different locations around the structures. Maximum values were employed to determine the structure stability. Figure 9 shows model-data comparison of dynamic pressures at 10 gauges installed in the vertical face and

underneath the caisson for Test 2. The numerical model is able to reproduce the amplitude and phase of the pressure oscillations at the vertical face of the caisson (Figures 9a-e). Moreover, model predictions show the dynamic pressure attenuation underneath the caisson toward the leeward side (Figures 9f-j). Larger discrepancies between data and predictions were found at P2 located near the still water line elevation (Figure 9b). Differences can be ascribed to model limitation to predict the free-surface elevation in front of the structure (Figure 8c-2).

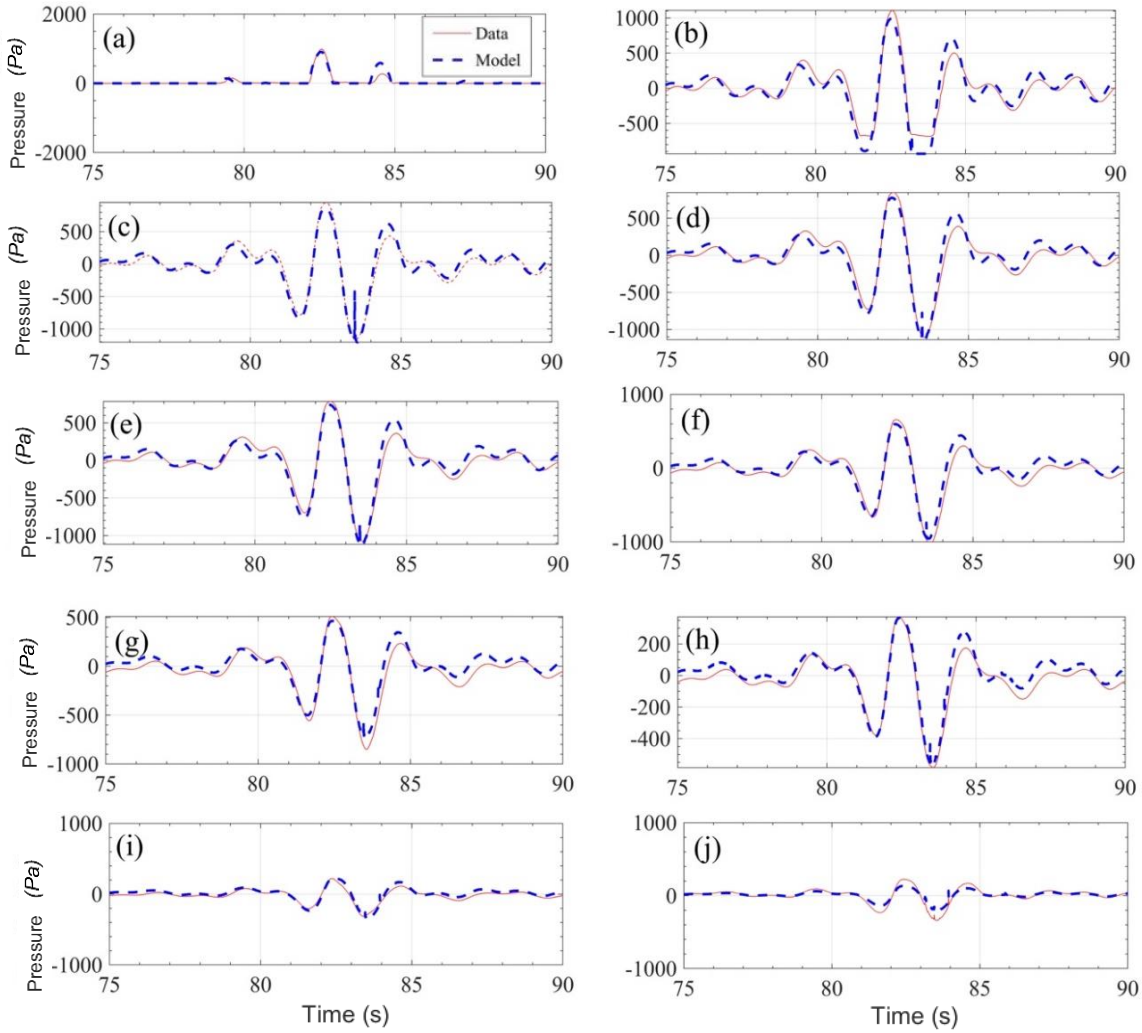

Figure 9. Model-data comparison of pressure time series at the vertical face (a: P1; b: P2; c: P3; d: P4; e: P5) and underneath (f: P6; g: P7; h: P8; i: P9; j: P10) the caisson. The locations of the pressure sensors are depicted in Figure 6.

Figure 10 and Table 5 present the model-data comparison for the maximum dynamic pressures. The numerical model unpredicts the maximum pressures recorded at P1 and P8.

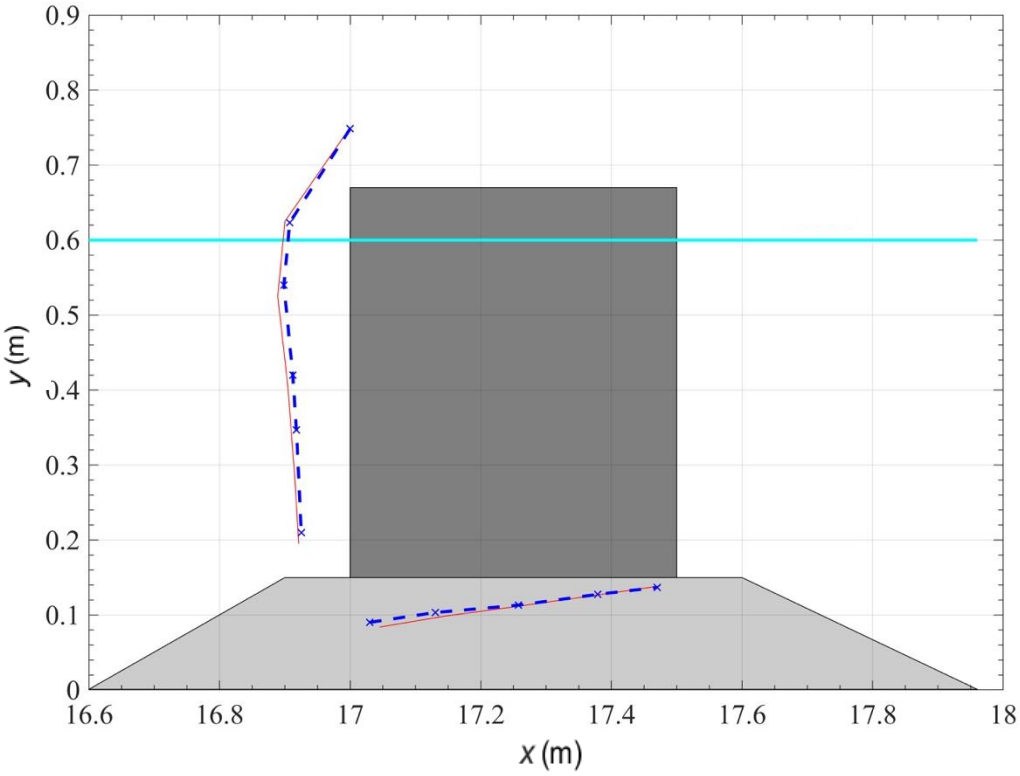

Figure 10. Distribution of wave pressure (data: solid line; predicted: dashed line) on a low mound-breakwater in Test 2 where 0.09 m represent 1 KPa.

Table 5. Absolute (E_A) and relative errors (E_R) between model and data for Test 2.

Sensor	Pressures Physical Model (*Pa*)	Pressures Numerical Model (*Pa*)	$E_a = \lvert P - P_{NM} \rvert$ (*Pa*)	$E_r = \left\lvert \frac{P - P_{NM}}{P} \right\rvert \times 100$ (%)
P1	998.76	908.00	90.76	9.09

P2	1 108.81	1 014.00	94.81	8.55
P3	954.10	878.00	76.10	7.98
P4	849.10	788	61.10	7.20
P5	787.21	748.00	39.21	4.98
P6	660.03	597.00	63.03	9.55
P7	514.80	466.00	48.80	9.48
P8	373.00	366.00	7.00	1.88
P9	224.00	223.00	1.00	0.45
P10	111.02	131.00	19.98	18.00
		Mean	50.18	7.71

The numerical model under prediction of the free-surface elevation in front of the structure explains the discrepancies in the pressure predictions. These results are consistent with Guanche (2007) who concluded that the construction of the low mound can influence the results. More specifically, small differences on both the geometry and the porous media characteristics between the numerical model and the physical model. Furthermore, differences in the wave generation method in the physical and numerical model can also affect the wave generation and propagation. The implementation of a moving paddle in the numerical model (e.g., Lara, Ruju, & Losada, 2010) can reduce such differences. Other sources of differences between the numerical model and the physical experiments are the limitation to absorb the incoming wave energy in dissipation areas in the wave flume (Alves-Oliveira, 2012).

Wave overtopping

The wave overtopping in the numerical model was estimated by free-surface elevation measurements at S17 located inside of the overtopping tank in Test 2. The overtopping volume is mainly ascribed to the wave focusing event. The model-data comparison shows a satisfacty agreement with a slightly smaller prediction (Figure 11 and Table 6).

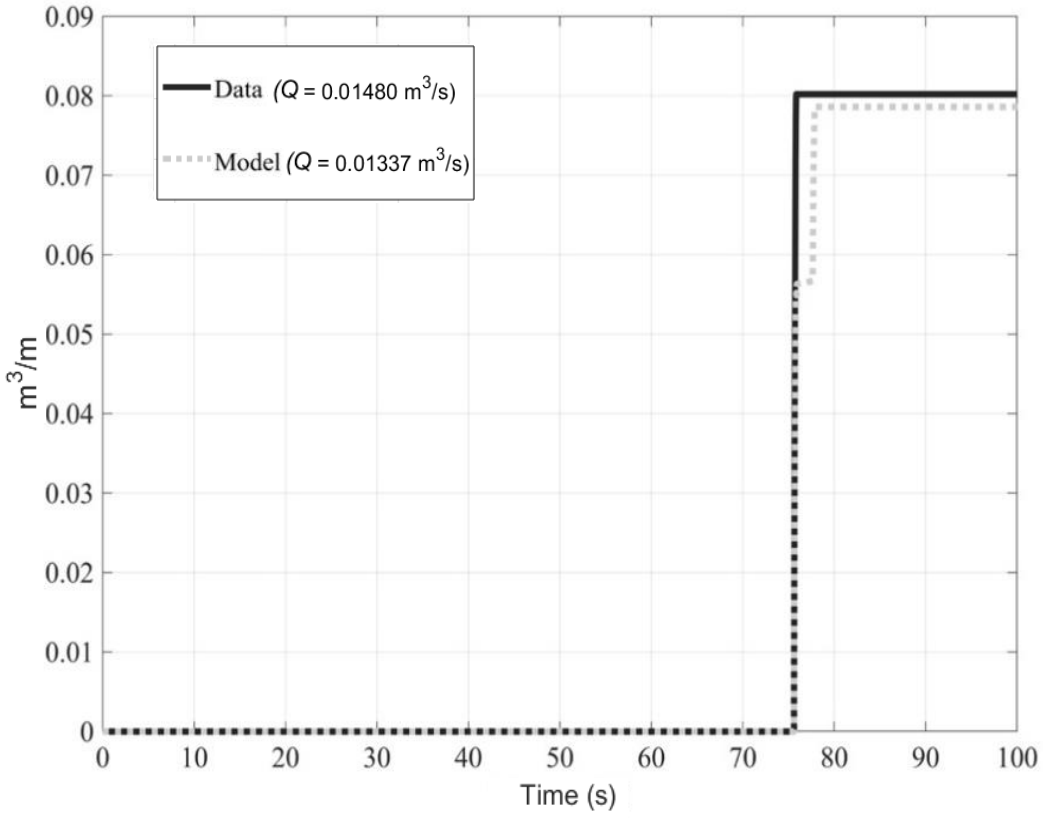

Figure 11. Model-data comparison of the instantaneous overtopping volume.

Table 6. Mean wave overtopping discharge and errors between physical model and numerical model prediction.

Test	Case	Wave type	Q Lab	Q Numerical model	$E_a = \|Q - Q_{NM}\|$	$E_r = \left\|\frac{Q-Q_{NM}}{Q}\right\| \times 100$ (%)
2	2	Transient wave group	0.014	0.013	0.001	9.66

Numerical model application

Model-data comparison demonstrated the model capability to simulate free-surface elevation, pressures, and overtopping associated to transient wave group interaction with a low mound breakwater (Figures 8-11). Here, we further employed the numerical model to investigate the wave-structure interaction sensitivity to the relative location of the structure with respect to the theoretical focusing location. The forcing conditions remain constant but the structure location is changed cross-shore to $x =$ 7 m, 14 m, 20 m, and 27 m (Table 2).

Figure 12 shows the dynamic pressures around the caisson for all the simulated cases. The maximum dynamic pressures present difference up to 14% depending on the structure location. It is worth to notice that maximum pressure at P10 during Case 3 (i.e., $x = 7$ m) is related to numerical noise. By ignoring this case we observe a similar trend for all simulated cases. On the other hand, wave overtopping presents larger differences between cases on the order of 45 % (Figure 13). The larger the constructive interference between individual waves, the larger the pressures (Figure 12) and overtopping (Figure 13). It is important to point out that the structure modified the wave focusing location due to wave reflection and hence equation (5) cannot be employed.

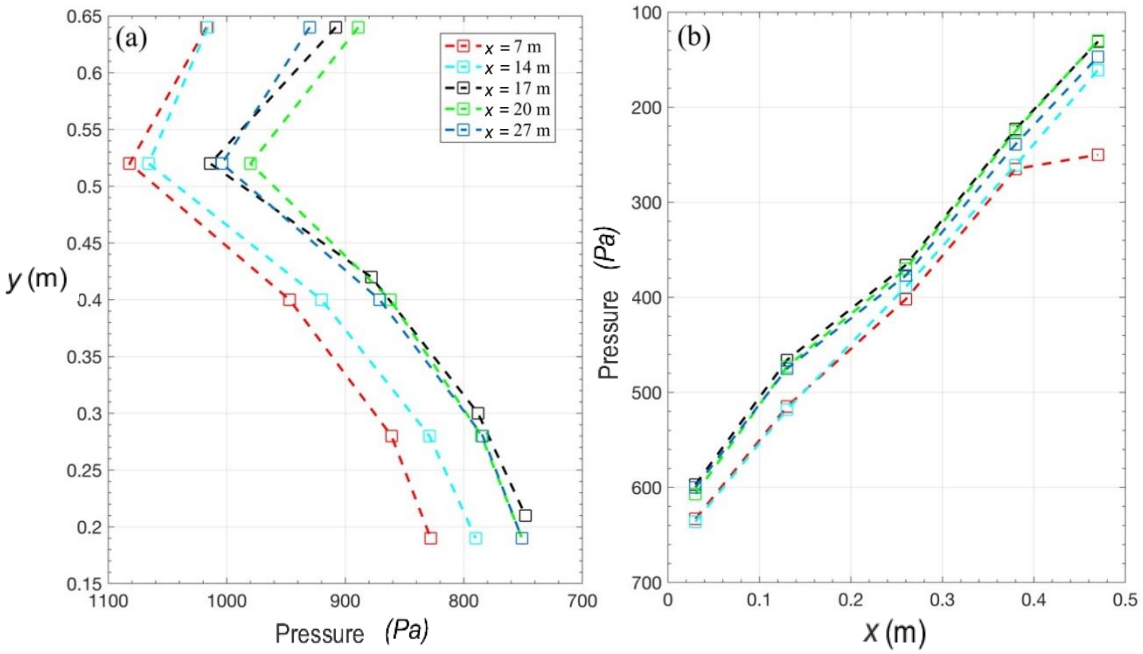

Figure 12. Distribution of dynamic pressure (a) along the vertical face and (b) underneath the caisson for different breakwater locations (Cases 2-6).

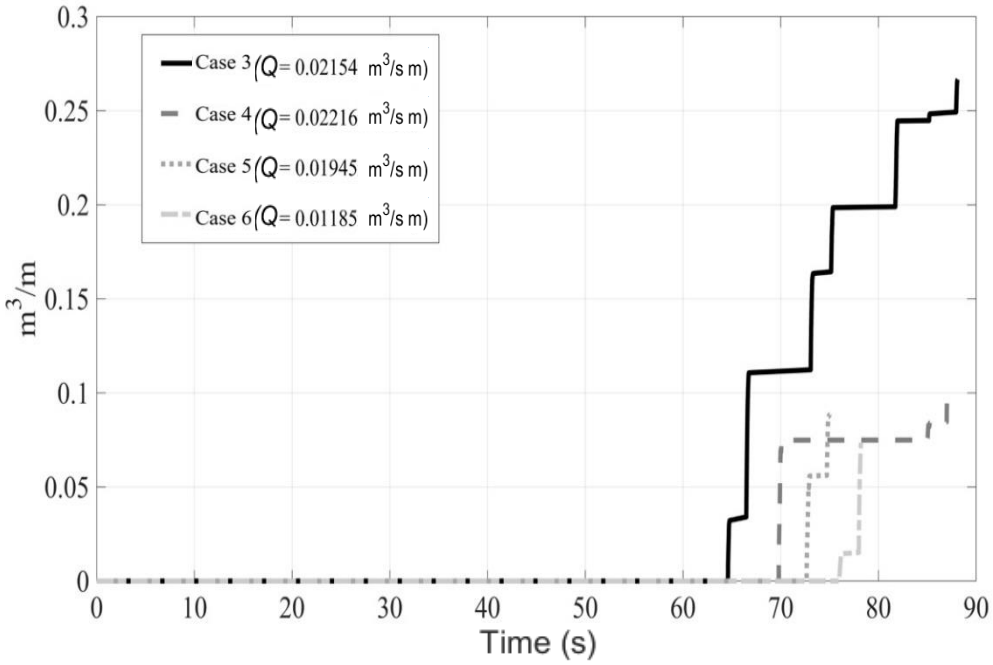

Figure 13. Instantaneous overtopping volume for: (a) Case 3, (b) Case 4, (c) Case 5, and (d) Case 6.

Discussion

The usefulness of semi-analytical and empirical formulation, widely employed for the design of coastal structures, are here assessed to

investigate transient wave group interaction with low mound breakwaters. We employed physical model pressures and overtopping measurements from Tests 2 and 3.

Dynamic pressures are calculated using the model proposed by Goda (1974). Model-data comparison shows that observations are under predicted for the two tests (Figure 14, Table 7 and Table 8). Moreover, wave overtopping prediction using the formulation from Franco and Franco (1999) also show an under prediction (Table 9). Therefore, semi empirical and parametric models are not able to reproduce complex wave transformation processes that were not considered during their derivation (Iribarren, 2013).

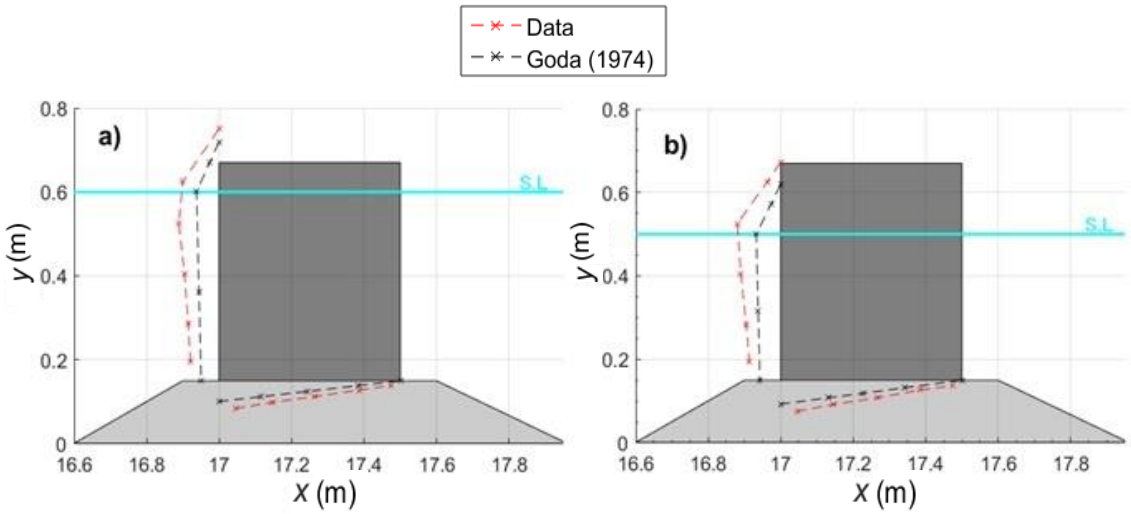

Figure 15. Distribution of wave pressure (data: red-dashed line; Goda model: black dashed line) on a low mound-breakwater for: (a) Test 2 and (b) Test 3. Notice that 0.09 m equals 1KPa.

Table 7. Absolute and relative errors of pressures between laboratory observations and Goda (1974) for Test 2.

Sensor	Pressures Lab (*Pa*)	Pressures Goda (1974) (*Pa*)	$E_a = \|P - P_{Goda}\|$ (*Pa*)	$E_r = \left\|\frac{P - P_{Goda}}{P}\right\| \times 100$ (%)
P1	998.76	0	998.76	100
P2	1 108.81	625.80	483.01	43.56
P5	787.21	492.30	294.91	37.46
P6	660.03	491.70	168.33	25.50
P10	111.02	17.50	93.52	84.23
		Mean	407.70	58.15

Table 8. Absolute and relative errors of pressures between laboratory observations and Goda (1974) for Test 3.

Sensor	Pressures Lab (*Pa*)	Pressures Goda (1974) (*Pa*)	$E_a = \|P - P_{Goda}\|$ (*Pa*)	$E_r = \left\|\frac{P - P_{Goda}}{P}\right\| \times 100$ (%)
P1	378.16	0	378.16	100
P2	1 195.99	673.2	522.79	43.71
P5	863.52	572.8	290.72	33.66
P6	747.80	571.9	175.90	23.52
P10	133.36	17.	115.86	86.87
		Mean	296.69	57.55

Table 9. Mean volume discharge computed by Franco and Franco (1999) and measured in the laboratory during Tests 2 and 3 with the corresponding absolute and relative errors.

Test	Wave type	*Q*Lab	*QA*	$E_a = \lvert Q - Q_{Franco} \rvert$	$E_r = \left\lvert \frac{Q - Q_{Franco}}{Q} \right\rvert \times 100$ (%)
2	Transient wave group	0.0148	0.000267	0.014533	98.19
3	Transient wave group	0	0.00000075	0.00000075	100

Conclusions

An integrated study of transient wave group interaction with a low mound breakwater was presented in this work. We employed physical laboratory experiments, RANS numerical simulations, and semi-analytical models. Based on the results the following conclusions were reached:

- The focusing wave point at intermediate water depth presented differences with respect to linear wave theory predictions. Such discrepancies can be ascribed to non-linear effects.

- The wave focusing location is highly sensitive to the presence of a breakwater owing to wave reflection.
- The RANS numerical model simulates the non-linear wave transformation of transient wave group interaction with a breakwater. The dynamic pressures were underestimated by 10%. Differences between the numerical model and observations are ascribed to difficulties in the numerical model to predict the free-surface elevation in front of the structure.
- The numerical model suggests differences of up to 14% and 45% for pressures and overtopping, respectively, ascribed to the relative structure location with respect to the theoretical wave focusing point.
- Semi-analytical and empirical models under predicted by 50% and 98% the pressures and overtopping, respectively, when wave focusing occurred.

Acknowledgments

We acknowledge to Sergio Camilo Rendón Valdez for proving technical support in the wave flume expriments. B. Rodrigo Covarrubias Contreras acknowledge CONACYT (No. 488695) for funding his graduate studies at UNAM. Alec Torres Freyermuth acknowledge DGAPA PAPIIT-UNAM IN101218 for financial support. Gonzalo Uriel Martín provided IT technical support. Two anonymous reviewers provided valuable comments to improve the manuscript.

References

Alves-Oliveira, T. C. (2012). *Generación de olas y estudio del rebase en un canal numérico de oleaje basado en el PFEM* (tesis doctoral). Universitat Politécnica de Catalunya, Cataluña, España.

Amarachaharam, T. (2016). *Numerical modelling of focussed wave hydrodynamics and focused wave-structure interaction with REEF3D* (master's thesis). Norwegian University of Science and Technology, Trondheim, Norway.

Baldock, T. E. (2006). Long wave generation by the shoaling and breaking of transient wave groups on a beach. *Proceedings of the Royal Society A: Mathematical, Physical and Engineering Sciences*, 462, 1853-1876.

Baldock, T. E., Swan, C., & Taylor, P. H. (1996). A laboratory study of non-linear waves on water. *Philosophical Transactions of the Royal Society A: Mathematical, Physical and Engineering Sciences*, 354, 649-676.

Chen, Q., Kirby, J. T., Dalrymple, R. A., Shi, F., & Thornton, E. B. (2003). Boussinesq modeling of longshore currents, *Journal of Geophysical Research*, 108(C11), 3362, DOI: 10.1029/2002JC001308.

Franco, C., & Franco, L. (1999). Overtopping formulas for caisson breakwaters with nonbreaking 3D waves. *Journal of Waterway, Port, Coastal, and Ocean Engineering, American Society of Civil Engineers*, 125(2), 98-108.

Goda, Y. (1974). New wave pressure formulae for composite breakwaters. *Proceedings of the 14th International Coastal Engineering Conference*, 3, 1702-1720.

Goda, Y. (2004). Spread parameter of extreme wave height distribution for performance-based design of maritime structures. *Journal of Waterway, Port, Coastal, and Ocean Engineering, American Society of Civil Engineers*, 130(1), 29-38.

Gornitz, V. (1991). Global coastal hazards from future sea level rise. *Palaeogrography, Palaeoclimatology, Palaeoecology*, 89(4), 379-398.

Guanche, R. (2007). *Análisis de la funcionalidad y estabilidad de obras marítimas mediante un modelo numérico basado en las ecuaciones de Reynolds* (tesis doctoral). Universidad de Cantabria, Cantabria, España.

Guanche, R., Losada, I., & Lara, J. (2009). Numerical analysis of wave loads for coastal structure stability. *Coastal Engineering*, 56(5-6), 543-558. DOI: 10.1016/j.coastaleng.2008.11.003

Higuera, P., Lara, J., & Losada, I. (2014). Three-dimensional interaction of waves and porous coastal structures using OpenFOAM®. Part II: Application. *Coastal Engineering*, (83), 259-270.

Hsu, T.-J., Sakakiyama, T., & Liu, P.-F. (2002). A numerical model for wave motions and turbulence flows in front of a composite breakwater. *Coastal Engineering*, 46, 25-50.

Iribarren, E. (2013). *Elementos para una nueva metodología de cálculo de diques verticales* (tesis doctoral). Universidad Politécnica de Madrid, Madrid, España.

Jiménez, C. (2010). *Criterios de diseño de rompeolas de berma, bajo el concepto de oleaje irregular* (tesis de maestría). Instituto Politécnico Nacional, México, D.F., México.

Kobayashi, N., & Wurjanto, A. (1992). Irregular wave set up and run-up on beaches. *Journal of Waterway, Port, Coastal, and Ocean Engineering*, 118, 368– 386.

Lara, J. L., García, N., & Losada, I. J. (2006). RANS modelling applied to random wave interaction with submerged permeable structures. *Coastal Engineering*, 53(5-6), 395-417.

Lara, J. L., Ruju, A., & Losada, I. J. (2010) Reynolds averaged Navier-Stokes modelling of long waves induced by a transient wave group on a beach. *Proceedings of the Royal Society A: Mathematical, Physical and Engineering Sciences*, (2011), 467, 1215–1242. Recovered from https://royalsocietypublishing.org/doi/pdf/10.1098/rspa.2010.0331

Li, M., Zhao, X., Ye, Z., Lin, W., & Chen, Y. (2018). Generation of regular and focused waves by using an internal wave maker in a CIP-based model. *Ocean Engineering*, 167, 334-347. Recovered from www.elsevier.com/locate/oceaneng

Lin, P., & Liu, P. L.-F. (1998). A numerical study of breaking waves in the surf zone. *Journal of Fluid Mechanics*, (359), 239-264.

Longuet-Higgins, M. (1974). Breaking waves - in deep or shallow water. *Proceedings of the Tenth Naval Hydrodynamics Symposium*, Office of Naval Research, 597-605.

Losada, I., Lara, J., Guanche, R., & González-Ondina, J. (2008). Numerical analysis of wave overtopping of high mound breakwaters. *Coastal Engineering*, (55), 47-62.

Nikolkina, I., & Didenkulova, I. (2011). Rogue waves in 2006-2010. *Natural Hazards and Earth System Sciences*, (11), 2913-2924.

Palemón-Arcos, L., Torres-Freyermuth, A., Chang, K.-A., Pastrana-Maldonado, D., & Salles, P. (2014). Modeling wave-structure interaction and its implication in offshore structure stability. *Proceedings of the Twentey-Foruth International Offshore and Polar Engineering Conference*, 1419-1424.

Palemón-Arcos, L., Torres-Freyermuth, A., Pedrozo-Acuña, A., & Salles, P. (2015). On the role of uncertainty for the study of wave–structure interaction. *Coastal Engineering*, 106, 32-41. Recovered from www.elsevier.com/locate/coastaleng

Rapp, R., & Melville, W. (1990). Laboratory measurements of deep-water breaking waves. *Philosophical Transactions of the Royal Society of London. Series A, Mathematical and Physical Sciences*, 331, 735-800. Recovered from royalsocietypublishing.org

Ryu, Y., & Chang, K. (2008). Green water void fraction due to breaking wave impinging and overtopping. *Experiments in Fluids*, 45(5), 883-898.

Stagonas, D., Buldakov, E., & Simons, R. (2018). Experimental generation of focusing wave groups on following and adverse-sheared currents in a wave-current flume. *Journal of Hydraulic Engineering*, 144(5), 1-11.

Torres-Freyermuth, A., Losada, I. J., & Lara, J. L. (2007). Modeling of surf zone processes on a natural beach using Reynolds-Averaged Navier-Stokes equations. *Journal of Geophysical Research*, 112, C09014.

Van-den-Boomgaard, M. (2003). *Wave focussing in a laboratory flume* (master's thesis). Technological University of Delft, Delft, The Netherlands.

Whittaker, C., Fitzgerald, C., Raby, A., Taylor, P., & Borthwick, A. (2018). Extreme coastal responses using focused wave groups: Overtopping and horizontal forces exerted on an inclined seawall. *Coastal Engineering*, 140, 292-305. Recovered from www.elsevier.com/locate/coastaleng

Whittaker, C., Fitzgerald, C., Raby, A., Taylor, P., Orszaghova, J., & Borthwick, A. (2017). Optimisation of focused wave group runup on a plane beach. *Coastal Engineering*, 121, 44–55. Recovered from www.elsevier.com/locate/coastaleng